Journal of Sound and Vibration (2002) **256**(4), 681–693
doi:10.1006/jsvi.5016, available online at http://www.idealibrary.com on IDEAL®

TOWARDS DEEP AND SIMPLE UNDERSTANDING OF THE TRANSCENDENTAL EIGENPROBLEM OF STRUCTURAL VIBRATIONS

F. W. WILLIAMS

Department of Building and Construction, City University of Hong Kong, Kowloon, Hong Kong

S. YUAN AND K. YE

Department of Civil Engineering, Tsinghua University, Beijing 100084, *People's Republic of China*

AND

D. KENNEDY AND M. S. DJOUDI

Cardiff School of Engineering, Cardiff University, Cardiff CF24 0YF, Wales. E-mail: kennedyd@cf.ac.uk

(*Received* 30 *May* 2001, *and in final form* 18 *January* 2002)

When using exact methods for undamped free vibration problems the generalized linear eigenvalue problem $(\mathbf{K}-\omega^2\mathbf{M})\mathbf{D}=\mathbf{0}$ of approximate methods, e.g., finite elements, is replaced by the transcendental eigenvalue problem $\mathbf{K}(\omega)\mathbf{D}=\mathbf{0}$. Here ω is the circular frequency; $\mathbf{D}$ is the displacement amplitude vector; $\mathbf{M}$ and $\mathbf{K}$ are the mass and static stiffness matrices; and $\mathbf{K}(\omega)$ is the dynamic stiffness matrix, with coefficients which include trigonometric and hyperbolic functions involving ω and mass because elements (for example, bars or beams) are analyzed exactly by solving their governing differential equations. The natural frequencies of this transcendental eigenvalue problem are generally found by the Wittrick–Williams algorithm which gives the number of natural frequencies below ω_t, a trial value of ω, as $\sum J_m + s\{\mathbf{K}(\omega_t)\}$ where $s\{\ \}$ denotes the readily computed sign count property of $\mathbf{K}(\omega)$ and the summation is over the clamped–clamped natural frequencies of all elements of the structure. Understanding the alternative solution forms of the transcendental eigenvalue problem is important both to accelerate convergence to natural frequencies, e.g., by plotting $|\mathbf{K}(\omega)|$, and to improve the mode calculations, which lack the complete reliability of natural frequencies obtained by using the Wittrick–Williams algorithm. The three solution forms are: $|\mathbf{K}(\omega)|=0$; $\mathbf{D}=\mathbf{0}$ with $|\mathbf{K}(\omega)|\to\infty$; and $|\mathbf{K}(\omega)|\neq 0$ with $\mathbf{D}\neq\mathbf{0}$. The literature covers the first two forms thoroughly but the third form has been almost totally ignored. Therefore, it is now examined thoroughly, principally by analytical studies of simple bar structures and also by confirmatory numerical results for a rigidly jointed plane frame. Although structures are unlikely to have exactly the properties giving this form, it needs to be understood, particularly because ill-conditioning can occur for structures approximating those for which it occurs.

1. INTRODUCTION

The undamped free vibration problems that often arise in structural analysis are generally solved by the finite element method (FEM) which leads to the usual linear eigenvalue problem

$$(\mathbf{K}-\omega^2\mathbf{M})\mathbf{D}=\mathbf{0}, \tag{1}$$

0022-460X/02/$35.00

where **K** is the static stiffness matrix and **D** is the modal displacement amplitude vector, such that the displacements are **D** sin ωt, where ω is the circular frequency and t is the time. Because the FEM involves discretization errors, the solutions obtained are only approximations to those of the problem being modelled. The accuracy can be increased by using more elements, which increases the order N of equation (1), but this is at the expense of additional computational effort and even then further work may be required if a measure of the accuracy to which the original physical problem has been solved is required. Therefore, it may be desirable to use "exact" methods which avoid the discretization errors of FEM whenever possible.

Such exact methods can be obtained whenever a structure can be divided into elements, which are then usually physical members of the structure, for which appropriate differential equations can be derived and solved—if necessary numerically rather than analytically. These differential equations include the distributed mass and stiffness of the member and give member equations relating the amplitudes of the forces and displacements at the ends of the members. The member dynamic stiffnesses are then assembled in exactly the same way as in FEM to obtain an overall dynamic stiffness matrix which will itself inevitably be a transcendental function of frequency. This results in the transcendental matrix equation

$$\mathbf{K}(\omega)\,\mathbf{D} = \mathbf{0}. \tag{2}$$

The only reliable solution of equation (2) is known to be found by application of the Wittrick–Williams (W–W) algorithm [1–3]. The algorithm states that J, the number of natural frequencies below ω_t, a trial value of ω, is given by

$$J = \sum J_m + s\{\mathbf{K}(\omega_t)\}, \tag{3}$$

where the summation is over all members; J_m is the number of natural frequencies of a member which would be exceeded by ω_t if its ends were to be clamped; and $s\{\mathbf{K}(\omega_t)\}$, the "sign count" of $\mathbf{K}(\omega_t)$, can be calculated as the number of negative elements on the leading diagonal of $\mathbf{K}(\omega_t)^{\Delta}$, where the superscript Δ denotes the upper triangular matrix obtained numerically from $\mathbf{K}(\omega_t)$ by the usual form of Gauss elimination, in which appropriate multiples of the pivotal row are subtracted from all (unscaled) succeeding rows and rows become pivotal in sequence. Equation (3) enables the development of many logical procedures (of which bisection is relatively simple but slow), for converging on any required natural frequencies by choosing appropriate successive values of ω_t, because J is known for every ω_t used. Hence the W–W algorithm of equation (3) requires $\mathbf{K}(\omega_t)$ to be assembled by solving the differential equations which govern the components of the structure. The algorithm also requires J_m to be found for each component member *from the same differential equations*.

The literature on solving generalized linear eigenproblems, i.e., equation (1), is extensive and thorough. It is instructive to use analogies between the linear and transcendental eigenvalue problems to enable the extensive work on the former to be used to elucidate and extend the far less extensive existing work on solving the transcendental eigenvalue problem. This requires the production of test problems of sufficient number and scope to test transcendental eigensolvers in all conceivable adverse circumstances.

The very simplest problems, which are more likely to occur in classroom examples than in real life, can produce some of the most demanding situations met by transcendental eigensolvers. Therefore, this paper mainly uses the very simplest of problems, involving only axial vibrations of an individual rod or of two collinear rods connected end to end. These

illustrate both the commonest and most obvious situation, for which $|\mathbf{K}(\omega)| = 0$, and the previously well-researched [2, 4, 5] alternative situation that $\mathbf{D} = \mathbf{0}$ and $|\mathbf{K}(\omega)| \to \infty$. More importantly, they include three cases of a previously unexamined possible situation, namely that natural frequencies occur for which $|\mathbf{K}(\omega)| \neq 0$ and $\mathbf{D} \neq \mathbf{0}$. Particular emphasis will be placed upon the consequences of this situation when finding both natural frequencies and modes of vibration. Nearly all the material presented will be new to most readers, who use FEM only, because the linear eigenproblem of equation (1) has no solutions except those for which $|\mathbf{K}(\omega)| = 0$.

The conclusions drawn from the thorough examination of simple rod problems are then stated more generally, so as to apply them to all structures. Emphasis is also placed on the possible ill-conditioning which can occur when the problem is close to being one of the special cases because real life problems are much more likely to fall into this category than to form a special case exactly.

2. SIMPLE ILLUSTRATIVE BAR EXAMPLES

The member equations for free axial vibration of a uniform bar are well known [6] to be

$$\begin{bmatrix} p_L \\ p_R \end{bmatrix} = hv \begin{bmatrix} \cot v & -\operatorname{cosec} v \\ -\operatorname{cosec} v & \cot v \end{bmatrix} \begin{bmatrix} u_L \\ u_R \end{bmatrix}, \tag{4}$$

where $h = EA/\ell$, $v = \omega\ell\sqrt{\mu/EA}$, ω is the circular frequency and the bar has length ℓ, mass per unit length μ, extensional rigidity EA, axial displacements $u_L \sin \omega t$ and $u_R \sin \omega t$ at its left-hand (L) and right-hand (R) ends (where t is the time) and corresponding end forces $p_L \sin \omega t$ and $p_R \sin \omega t$.

With F and C, respectively, denoting free and clamped ends, the natural frequencies for the F–F, C–C and F–C combinations of end conditions are also well known to be, for $i = 1, 2, 3, \ldots$,

$$\text{(F–F)} \qquad v = 0 \text{ or } i\pi, \tag{5}$$

$$\text{(C–C)} \qquad v = i\pi, \tag{6}$$

$$\text{(F–C)} \qquad v = (i - \tfrac{1}{2})\,\pi. \tag{7}$$

Equations (4)–(7) can be derived very easily, for $v > 0$, from the governing differential equation of motion

$$EA\, U'' - \mu \ddot{U} = 0 \tag{8}$$

in which an over-dot represents differentiation with respect to time and a prime denotes differentiation with respect to the longitudinal co-ordinate x. Hence equations (4)–(7) follow by substituting $U = u(x) \sin \omega t$ and imposing the appropriate boundary conditions at $x = 0$ and ℓ. Thus, equation (4) is given by $u(0) = u_L$, $u(\ell) = u_R$, $EA\, u'(0) = -p_L$, $EA\, u'(\ell) = p_R$; equations (5)–(7) are given by $u'(0) = u'(\ell) = 0$; $u(0) = u(\ell) = 0$; and $u'(0) = 0$, $u(\ell) = 0$ respectively. Note that all of these derivations involve u varying sinusoidally with x, with half-wavelength $\pi\ell/v$.

For simplicity, a single member may be considered as the full structure. Therefore, a single bar is examined below, first with F–C end conditions and then with F–F ones.

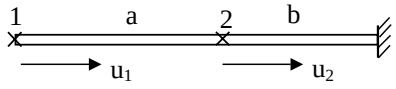

Figure 1. Simple two-bar structure, consisting of the collinear bars a and b, with b clamped at its right-hand end and a free at its left-hand end.

For the F–C case, the overall stiffness matrix for the simple structure is obtained from equation (4) by setting $u_R = 0$. Hence, it is a (1×1) matrix, i.e., the scalar $hv \cot v$. Therefore, $|\mathbf{K}(\omega)| = 0$ when $\cot v = 0$, i.e., at $v = (i - \frac{1}{2})\pi$. This agrees with equation (7) and is therefore the correct result. Thus, this case represents the usual situation in which $|\mathbf{K}(\omega)| = 0$ gives the natural frequencies, i.e., the eigenvalues.

For the F–F case, equation (4) is the stiffness formulation for the whole structure. Hence, $|\mathbf{K}(\omega)| = h^2v^2(\cot^2 v - \operatorname{cosec}^2 v) = -h^2v^2$. Hence, not only is this a case where $|\mathbf{K}(\omega)| \neq 0$ but it is also a highly unusual situation in which $|\mathbf{K}(\omega)|$ varies linearly with v^2, and hence with ω^2. Thus, this simplest of all possible structures has thrown up what is probably the most unusual special case of all! However, it is very important to note that even such a special case causes no problems when using the (W–W) algorithm, as follows.

From equation (4),

$$\mathbf{K}(\omega)^A = hv \begin{bmatrix} \cot v & -\operatorname{cosec} v \\ 0 & -\tan v \end{bmatrix} \tag{9}$$

in which element (2,2) is a simplification of $(\cot v - \operatorname{cosec}^2 v/\cot v)$. Hence, the two leading diagonal elements of $\mathbf{K}(\omega)^A$ are always of opposite sign and so $s\{\mathbf{K}(\omega)\} = 1$ for all values of ω. (Strictly, they are not of the opposite sign when $\cot v = 0$ but then $\tan v \to \infty$ and so computation is impossible. Similarly when $\tan v = 0$, $\cot v \to \infty$.) Hence, the W–W algorithm of equation (3) gives $J = \sum J_m + 1$ for all values of ω, so that $J = 1$ if ω is infinitesimally greater than zero. Therefore the natural frequencies are given by 0 and the natural frequencies of the C–C case. Using equation (6), this means that the natural frequencies have been correctly predicted as those given by equation (5).

The simple two-bar structure of Figure 1 is now considered. It has $\mathbf{D} = [u_1 \quad u_2]^T$ and, using equation (4),

$$\mathbf{K}(\omega) = \begin{bmatrix} (hv \cot v)_a & (-hv \operatorname{cosec} v)_a \\ (-hv \operatorname{cosec} v)_a & (hv \cot v)_a + (hv \cot v)_b \end{bmatrix}, \tag{10}$$

where the subscripts denote properties of bars a and b, so that

$$\mathbf{K}(\omega)^A = \begin{bmatrix} (hv \cot v)_a & (-hv \operatorname{cosec} v)_a \\ 0 & (hv \cot v)_b - (hv \tan v)_a \end{bmatrix} \tag{11}$$

in which $-(hv \tan v)_a$ is a simplification of $(hv \cot v - hv \operatorname{cosec}^2 v/\cot v)_a$. Denoting the leading diagonal elements of $\mathbf{K}(\omega)^A$ by

$$k_{11}^A = (hv \cot v)_a, \tag{12}$$

$$k_{22}^A = (hv \cot v)_b - (hv \tan v)_a, \tag{13}$$

equation (11) gives

$$|\mathbf{K}(\omega)| = k_{11}^A k_{22}^A = (hv \cot v)_a (hv \cot v)_b - (hv)_a^2 . \tag{14}$$

When $\mathbf{D} = \mathbf{0}$, the structure degenerates into two bars with their ends clamped and hence equation (6) gives

$$\sum J_m = int\{v_a/\pi\} + int\{v_b/\pi\}, \tag{15}$$

where $int\{\ \}$ denotes the highest integer that does not exceed the value of the expression within the brackets. Additionally, from equation (11),

$$s\{\mathbf{K}(\omega)\} = s\{k_{11}^A\} + s\{k_{22}^A\}, \tag{16}$$

where $s\{\ \} = 1$ if the expression within the brackets is negative, otherwise $s\{\ \} = 0$.

By substituting equations (15) and (16) into the W–W algorithm of equation (3),

$$J = int\{v_a/\pi\} + int\{v_b/\pi\} + s\{k_{11}^A\} + s\{k_{22}^A\}. \tag{17}$$

Thus J is the sum of four non-negative components. The following discussion (in which i and j are any positive integers) explains how these components vary as ω, and hence also v_a and v_b, are increased from zero, for the various cases illustrated in Figure 2. In each of Figures 2(a) and 2(b), which represent structures with different member properties, the upper plot shows the variation of k_{11}^A and k_{22}^A with v_a and v_b, while the lower plot shows the corresponding variation of J and its components.

(i) When $(hv \cot v)_b = (hv \tan v)_a$, k_{22}^A decreases through zero so that $s\{k_{22}^A\}$ increases by one. Equation (17) shows that J increases by one, and so the W–W algorithm indicates that there is a single natural frequency there for which equation (14) gives $|\mathbf{K}(\omega)| = 0$. Hence, this is an example of the commonest situation, in which $|\mathbf{K}(\omega)| = 0$ gives the natural frequencies; see for example the points denoted ω_1 and ω_2 in Figures 2(a) and 2(b).

(ii) When $v_a = (i - \frac{1}{2})\pi$, $\cot v_a$ decreases through zero and $\tan v_a$ simultaneously goes through $\mp\infty$. Thus equations (12) and (13) show that $s\{k_{11}^A\}$ increases by one and $s\{k_{22}^A\}$ decreases by one. Such points are labelled as case A in Figures 2(a) and 2(b). Equation (14) shows that $|\mathbf{K}(\omega)| = -(hv)_a^2 \neq 0$. More importantly, equation (17) shows that J is unchanged and so the W–W algorithm shows that there is not a natural frequency of the structure at $v_a = (i - \frac{1}{2})\pi$, except in the special case considered in (iv) below.

(iii) When $v_a = i\pi$, $\cot v_a$ goes through $\mp\infty$. Thus equation (12) shows that $s\{k_{11}^A\}$ decreases by one. But $int\{v_a/\pi\}$ simultaneously increases by one so that J is unchanged. Similarly when $v_b = j\pi$, $s\{k_{22}^A\}$ decreases by one and $int\{v_b/\pi\}$ increases by one so that J is unchanged. These two situations are labelled as case B in Figures 2(a) and 2(b) respectively. Equation (14) shows that such points give poles in the plot of $|\mathbf{K}(\omega)|$, which are distinct from the natural frequencies given by (i) above except in the special cases considered in (iv) and (v) below.

(iv) Now consider the exceptional circumstance in which $v_a = (i - \frac{1}{2})\pi$ and $v_b = j\pi$ at the same frequency ω, as illustrated by case C in Figure 2(a). The definitions associated with equation (4) show that this will happen if the properties of bars a and b are such that

$$(EA/\mu\ell^2)_b = \{(i - \tfrac{1}{2})/j\}^2 (EA/\mu\ell^2)_a\,. \tag{18}$$

At frequency ω, $s\{k_{11}^A\}$ increases by one, while both terms of k_{22}^A pass through $\mp\infty$ so that $s\{k_{22}^A\}$ decreases by one. Also, $int\{v_b/\pi\}$ increases by one, resulting in a net increase of one in J, which indicates the presence of a single natural frequency ω^*. Now $\mathbf{D} \neq \mathbf{0}$,

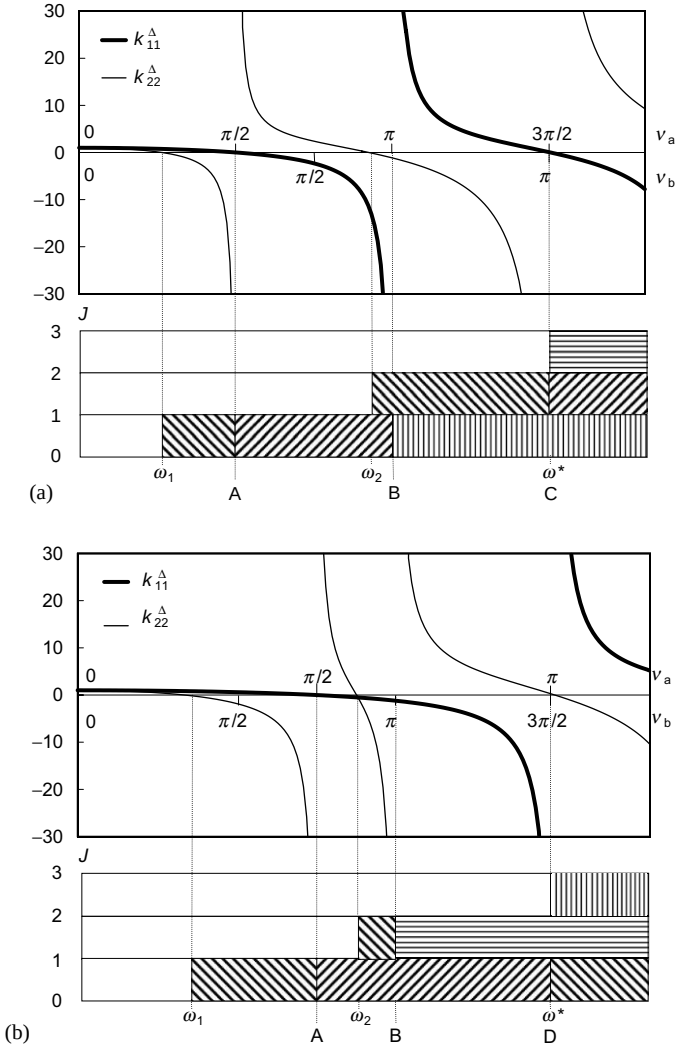

Figure 2. Variation of J and its components with ω (and hence with v_a and v_b), for the structure of Figure 1 with member properties resulting in $h_a = h_b = 1$ and (a) $v_a = 1{\cdot}5v_b$; (b) $v_b = 1{\cdot}5v_a$. The shading in the lower plots indicates regions where (▥) $int\{v_a/\pi\} = 1$; (▤) $int\{v_a/\pi\} = 1$; (▨) $s\{k^A_{11}\} = 1$; (▧) $s\{k^A_{22}\} = 1$. ω_1, ω_2 and ω^* are natural frequencies. A–D denote the cases described in section 2.

because the absence of an axial force at the free node 1 in Figure 1 requires $u'_1 = 0$, which would be incompatible with $u_1 = 0$ due to the sinusoidal variation of the longitudinal displacement. Applying a limiting process to equation (14) gives

$$|\mathbf{K}(\omega^*)| = -(i - \tfrac{1}{2})^2\pi^2 h_a(h_a + h_b) \neq 0. \tag{19}$$

Hence, case C is an example of the situation for which $|\mathbf{K}(\omega)| \neq 0$ and $\mathbf{D} \neq \mathbf{0}$ at the natural frequency. Note that case C only occurs if equation (18) is satisfied. Hence, if it occurs for $(i = 1, j = 2)$ it will also occur for $(i = 2, j = 6)$ but not for $(i = 2, j = 3)$, etc.

(v) Finally, suppose that the properties of bars a and b are chosen such that $v_a = i\pi$ and $v_b = (j - \frac{1}{2})\pi$ at the same frequency ω, as illustrated by case D in Figure 2(b). This will

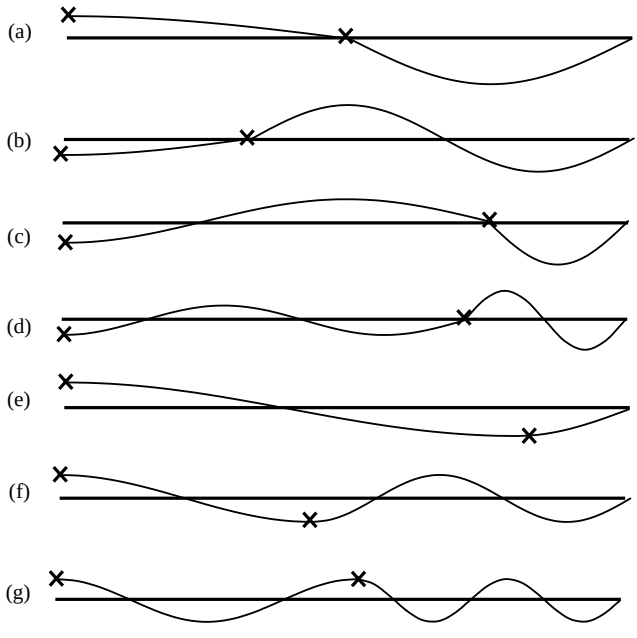

Figure 3. Selected mode shapes for case C, satisfying equation (18) with (a) ($i = 1$, $j = 1$); (b) ($i = 1$, $j = 2$); (c) ($i = 2$, $j = 1$); (d) ($i = 3$, $j = 2$); and for case D, satisfying equation (20) with (e) ($i = 1$, $j = 1$); (f) ($i = 1$, $j = 3$); (g) ($i = 2$, $j = 4$). Crosses indicate nodes 1 and 2 shown in Figure 1.

happen if

$$(EA/\mu\ell^2)_b = \{i/(j - \tfrac{1}{2})\}^2 (EA/\mu\ell^2)_a . \tag{20}$$

Here, cot v_a passes through $\mp \infty$ so that $s\{k^A_{11}\}$ decreases by one, while both terms of k^A_{22} decrease through zero so that $s\{k^A_{22}\}$ increases by one. Also, $int\{v_a/\pi\}$ increases by one, giving a net increase of one in J and so indicating the presence of a single natural frequency ω^*. Now $\mathbf{D} \neq \mathbf{0}$, for the same reason as that given in (iv) above for case C, and a limiting process gives

$$|\mathbf{K}(\omega^*)| = -h_a \pi^2 \{i^2 h_a + (j - \tfrac{1}{2})^2 h_b\} \neq 0. \tag{21}$$

Thus, case D also represents the unexpected situation of natural frequencies occurring for structures for which neither $|\mathbf{K}(\omega)| = 0$ nor $\mathbf{D} = \mathbf{0}$.

Figure 3 illustrates, for $\mu_b = \mu_a$ and $EA_b = \frac{1}{4}EA_a$, typical mode shapes for cases C and D considered above, i.e., the two cases for which $|\mathbf{K}(\omega)| \neq 0$ and $\mathbf{D} \neq \mathbf{0}$ at the natural frequency. The sine waves shown are not deflected shapes nor are the straight lines the bar structure of Figure 1. Instead, the sine waves represent the variation of the axial displacement U along the length of the bar with half-wavelength $\pi\ell/v$ (see the note below equation (8)), and the straight line is the axis of the sine wave. It can be seen that case C represents bar a vibrating as an F–C bar while bar b provides the equilibrium force required at node 2 by vibrating as a C–C bar. Case D consists of bar a vibrating as an F–F bar while bar b vibrates as an F–C bar but with its displacement at node 2 compatible with bar a. Note that the half-wavelengths of the sine waves will not be the same for bars a and b in either of the cases C and D except for the special case of bars a and b having identical

values of ℓ/v, and hence also of EA/μ. Note also that for case C the slopes of the sine waves to the left and right of node 2 will usually be different as a consequence of the clamping forces at node 2 needing to be equal when the bars on either side of node 2 are not.

3. EFFECT ON MODE FINDING

A simple but effective method [7] for obtaining modes of vibration to better than engineering accuracy, quite widely reported in the literature [4, 5, 8], has been shown to be solving equation (2) with its null right-hand side replaced by a random vector $\mathbf{P}_R$ and with ω close to the corresponding natural frequency. The reasoning that yielded this method is that if a real structure is excited by any load system with a frequency close to one of its natural frequencies, the response is dominated by the corresponding mode. This *random force method* has been validated in the literature by solving problems, including identified special cases, numerically although the special cases of the present paper have not all been included. However, the simplicity of the examples given in the previous section enables instead the method to be evaluated analytically, as follows.

For the very special case of the single F–F bar of equation (9), $\mathbf{P}_R$ can be represented by

$$\mathbf{P}_R = [P_1 \quad P_2]^{\mathrm{T}}, \tag{22}$$

which is modified by the forward Gauss elimination step which gave equation (9) to become $[P_1 \;\; P_2 + P_1 \sec v]^{\mathrm{T}}$, where sec v is a simplification of cosec v/cot v. Because ω is close to one of the natural frequencies given by equation (5), $v = i\pi - i\pi\varepsilon(\varepsilon \to 0)$ and so by using $\tan v \cong -i\pi\varepsilon$, $-\sin v \cong \mp i\pi\varepsilon$, $\sec v \cong \mp 1$, this modified vector couples with equation (9) to give

$$h \begin{bmatrix} -1/i\pi\varepsilon & \mp 1/i\pi\varepsilon \\ 0 & i\pi\varepsilon \end{bmatrix} \begin{bmatrix} D_1 \\ D_2 \end{bmatrix} = \begin{bmatrix} P_1 \\ P_2 \mp P_1 \end{bmatrix}, \tag{23}$$

where the $\mp$ signs are negative (positive) when i is odd (even). Hence back-substituting and retaining only first order terms gives the mode as $[D_1 \;\; D_2]^{\mathrm{T}} = [\mp (P_2 \mp P_1)/i\pi\varepsilon h \;\; (P_2 \mp P_1)/i\pi\varepsilon h]^{\mathrm{T}}$ which after normalization is the correct mode $D_1 = -D_2 = 1$ for i odd or $D_1 = D_2 = 1$ for i even. Hence, back-substitution into the differential equation for the bar, see equation (8), shows that the former are symmetric modes with U varying with an odd number of sinusoidal half-wavelengths along the bar and a nodal point at its centre, while the latter are antisymmetric modes with an even number of half-wavelengths with maxima at the ends and centre of the bar, as well as elsewhere for $i \geqslant 4$.

Equation (22) also represents a random force vector for the two-bar problem corresponding to equation (10). Hence the right-hand side corresponding to the $\mathbf{K}(\omega)^{\Delta}$ of equation (11) is $[P_1 \;\; P_2 + P_1 \sec v_a]^{\mathrm{T}}$. Therefore, substituting $v_a = (i - \frac{1}{2})\pi - (i - \frac{1}{2})\pi\varepsilon$ and $v_b = j\pi - j\pi\varepsilon$ into equation (11) gives

$$\begin{bmatrix} h_a(i-\frac{1}{2})\pi(i-\frac{1}{2})\pi\varepsilon & \mp h_a(i-\frac{1}{2})\pi \\ 0 & \{h_a(i-\frac{1}{2})\pi/(i-\frac{1}{2})\pi\varepsilon\} - h_b j\pi/j\pi\varepsilon \end{bmatrix} \begin{bmatrix} D_1 \\ D_2 \end{bmatrix} = \begin{bmatrix} P_1 \\ P_2 \pm P_1/(i-\frac{1}{2})\pi\varepsilon \end{bmatrix} \tag{24}$$

for case C. Similarly, substituting $v_a = i\pi - i\pi\varepsilon$ and $v_b = (j - \frac{1}{2})\pi - (j - \frac{1}{2})\pi\varepsilon$ gives

$$\begin{bmatrix} -h_a i\pi/i\pi\varepsilon & \mp h_a i\pi/i\pi\varepsilon \\ 0 & h_a i\pi i\pi\varepsilon + h_b(j-\frac{1}{2})\pi(j-\frac{1}{2})\pi\varepsilon \end{bmatrix} \begin{bmatrix} D_1 \\ D_2 \end{bmatrix} = \begin{bmatrix} P_1 \\ P_2 \mp P_1 \end{bmatrix} \tag{25}$$

for case D. Again the $\mp$ signs are negative (positive) when i is odd (even) and the $\pm$ sign is positive (negative) for i odd (even).

It is readily deduced from equations (24) and (25) that the normalized modes for cases C and D are $[1 \quad 0]^T$ and $[1 \quad \mp 1]^T$ respectively. These two modes are correct, and back-substitution into the differential equations of bars a and b (see equation (8) and the note below it that the longitudinal half-wavelength is $\pi\ell/v$) gives modes such as those shown in Figure 3. However, it should be noted that except for special cases (such as when a and b form a continuous uniform cantilever into which node 2 has been unnecessarily inserted such that, for $i = j = 1$, $\ell_a = \frac{1}{2}\ell_b$ in case C or $\ell_a = 2\ell_b$ in case D), the half-wavelength of the sine wave for bar a differs from that of bar b because their values of ℓ/v differ, as Figure 3 illustrates.

From equation (25) the choice of $P_2 = \pm P_1$ is clearly inappropriate for case D. Because the choice of the right-hand side should be random, this possibility is very unlikely to occur, although it might unwisely be used in a classroom example! Taking the appropriate extra second order terms in the expansions which gave equation (25) and considering the case $i = j = 1$ and $h_b = 2h_a$ gives the incorrect mode $[D_1 \quad D_2]^T = [1 \quad \frac{1}{2}]^T$. In detail, consider the limit as $\varepsilon \to 0$ when $P_2 \cong P_1$, by using $P_2 = P_1(1 - \gamma)$ with γ small. Now the multiplier used when obtaining equation (25) is given by equation (10) as sec v_a, which approximates to $-(1 + \frac{1}{2}\pi^2\varepsilon^2)$ so that the $P_2 - P_1$ of equation (25) becomes $P_1(-\gamma - \frac{1}{2}\pi^2\varepsilon^2)$. Hence equation (25) gives

$$D_2 = P_1(-\gamma - \tfrac{1}{2}\pi^2\varepsilon^2)/\{\varepsilon\pi^2(h_a + \tfrac{1}{4} \times 2h_a)\}, \tag{26}$$

$$D_1 = -\{P_1 + (h_a/\varepsilon)D_2\}/(h_a/\varepsilon) = -\{D_2 + \varepsilon P_1/h_a\}$$

$$= -D_2\left\{1 - \frac{3}{2}\left(\frac{\varepsilon^2\pi^2}{\gamma + \frac{1}{2}\pi^2\varepsilon^2}\right)\right\}. \tag{27}$$

For $\gamma = 0$, this gives the incorrect mode $D_1 = 2D_2$ reported above. However for $\gamma \gg \varepsilon^2$, it gives $D_1 \cong -D_2(1 - 3\varepsilon^2\pi^2/2\gamma) \cong -D_2$, so that the correct mode is approached as $\varepsilon \to 0$ and the percentage error $\cong 100 \times 3\varepsilon^2\pi^2/2\gamma$. Hence, for the eigenvalue accuracy of $\varepsilon \cong 10^{-6}$ usually recommended for use with the random force vector mode finding method, the error in the mode is approximately $(100 \times 3 \times 10^{-11}/2\gamma)\%$. Hence, a mode accuracy of 0·1%, which usually suffices in engineering, is obtained for $\gamma \geqslant 1{\cdot}5 \times 10^{-8}$. Thus there is a well below one in ten million chance of the random force vector method failing to achieve engineering accuracy for this example.

4. ILL-CONDITIONING IN THE VICINITY OF SPECIAL CASES

It has been shown in equations (19) and (21) that $|\mathbf{K}(\omega^*)| \neq 0$ at the natural frequency ω^* of either case C or case D. However, cases C and D are, respectively, special cases of A and B, which have $|\mathbf{K}(\omega)| = 0$ at all natural frequencies. Hence, if L_a and L_b are the values of ℓ_a and ℓ_b giving cases C or D, altering these lengths to $L_a + \delta L_a$ and $L_b - \delta L_a$, where δL_a is a tiny ("almost infinitesimal") amount, will result in $|\mathbf{K}(\omega^*)|$ being zero instead of non-zero at the natural frequency. This suggests that if plots of $|\mathbf{K}(\omega)|$ versus ω are plotted on a single graph for various values of δL_a the graph must have one of the two forms shown exaggeratedly in Figure 4, in which the shape of the curve for $\delta L_a = 0$ has been assigned arbitrarily.

To check this intuitive conclusion, computer runs were performed with $\delta L_a = 0$, $\delta L_a = 0{\cdot}001\ell_a$, $\delta L_a = 0{\cdot}002\ell_a$ and $\delta L_a = 0{\cdot}003\ell_a$ for both of cases C and D, with

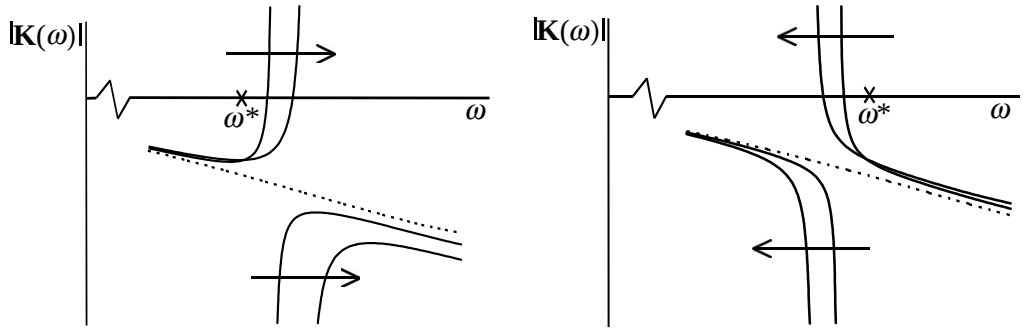

Figure 4. $|\mathbf{K}(\omega)|$ versus ω plots for examples approximating cases C and D. The dashed curve is for $\delta L_a = 0$ and the continuous curves are for two values of δL_a, with the arrows indicating progression from the lower to the higher of the two values. Note that the continuous curves can cross, as shown, due to the natural frequency and the pole (= vertical asymptote) moving as δL_a increases.

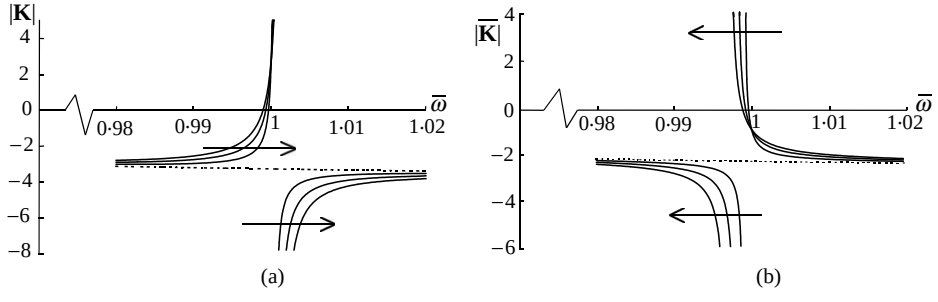

Figure 5. Plots of $|\bar{\mathbf{K}}|$ versus $\bar{\omega}$ for: (a) case C ($i = 2$, $j = 3$); (b) case D ($i = 5$, $j = 3$). Key: $\bar{\omega} = \omega/\omega^*$, $|\bar{\mathbf{K}}| = |\mathbf{K}(\omega)| \times 10^{-m}$ where (a) $m = 7$; (b) $m = 8$. The arrows indicate progression from the lowest to the highest values of δL_a, the three values used being $\delta L_a/L_a = 0{\cdot}001$, $0{\cdot}002$ and $0{\cdot}003$. The curve for $\delta L_a/L_a = 0$ is shown dashed.

$EA_b = 2{\cdot}88EA_a$, $\mu_b = 2\mu_a$, $i = 2$ and $j = 3$ for case C so that equation (18) gives $L_b = 2{\cdot}4L_a$; and with $EA_b = 0{\cdot}845EA_a$, $\mu_b = 0{\cdot}5\mu_a$, $i = 5$ and $j = 3$ for case D so that equation (20) gives $L_b = 0{\cdot}65L_a$. The results of Figure 5 were obtained by using $EA_a = 1200$, $\mu_a = 0{\cdot}263$ and $L_a = 1{\cdot}47$.

From these results it is obvious that when δL_a is small, any attempt to converge on the natural frequency by following the $|\mathbf{K}(\omega)|$ versus ω curve will at best be very slow and at worst will suffer ill-conditioning, although so long as the W–W algorithm is used at every ω_t and adequate recovery procedures are included, such as reverting to bisection, the natural frequency should still eventually be converged on.

5. OTHER CASES FOR WHICH $|\mathbf{K}(\omega)| \neq 0$ AND $\mathbf{D} \neq \mathbf{0}$ AT A NATURAL FREQUENCY

There is a complete analogy between the torsional vibration of a shaft of length ℓ and the axial vibration of a bar of length ℓ. Hence, if GJ is the torsional rigidity of the shaft and I_p is its polar moment of inertia, the results of sections 2–4 apply to shafts so long as EA and μ are replaced by GJ and I_p, so that $h = GJ/\ell$ and $v = \omega\ell\sqrt{I_p/GJ}$ [6]. There is also a complete mathematical analogy between vibrating bars and vibration of taut strings [6],

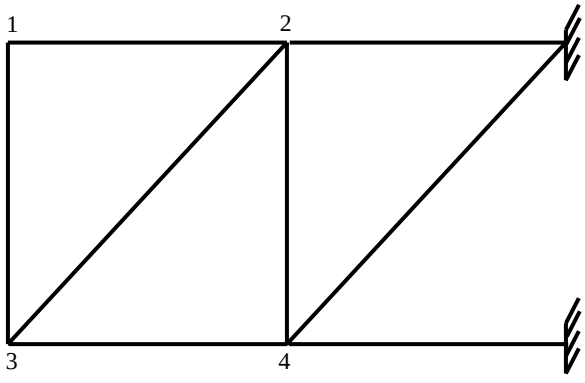

Figure 6. Rigidly jointed plane frame built-in at its right-hand boundary. $L = 3$ m for the horizontal and vertical members. The diagonal member 2–3 has $EA = 10^3$ MN, $EI = 1$ MN m^2 and $\mu = 100$ kg/m. All the other members have $EA = 10^3\alpha$ MN, $EI = \alpha$ MN m^2 and $\mu = 100$ kg/m.

but this is of little or no relevance because at least one end is free in sections 2–4 and it is unclear how tension could be applied at the free end of a string.

The above examples are still very simple, so the question arises as to whether the situation for which $|\mathbf{K}(\omega)| \neq 0$ and $\mathbf{D} \neq \mathbf{0}$ at a natural frequency can ever arise for more complicated structures. Because, as expected, the W–W algorithm fully explained the special cases given above, it can also be used to answer this question positively and in a completely general way, as follows.

Consider a structure of any complexity whatsoever that has $N_f (\geqslant 1)$ natural frequencies at $\omega = \omega^*$ when clamps are used to enforce $\mathbf{D} = \mathbf{0}$ so that $\sum J_m$ increases by N_f as ω is increased through ω^*. Suppose that the actual (unclamped) structure also has N_f natural frequencies at ω^*, so that J also increases by N_f as ω is increased through ω^*. It follows from the W–W algorithm of equation (3) that $s\{\mathbf{K}(\omega)\}$ does not change value as ω is increased through ω^*. Now it is known [7] that as ω is increased the leading diagonal elements of $\mathbf{K}(\omega)^A$ can only change sign *either* from $-$ to $+$ via infinity *or* from $+$ to $-$ through zero. Therefore, the number of diagonal elements of $\mathbf{K}(\omega)^A$ that approach zero as $\omega \to \omega^*$ must be equal to the number that approach infinity, so that $|\mathbf{K}(\omega)|$, the product of the leading diagonal terms of $\mathbf{K}(\omega)^A$, must be finite at $\omega = \omega^*$. This means, for example, that if a plane frame has a natural frequency ω^* at exactly a C–C natural frequency of one of its members, and if none of its other members shares that C–C natural frequency, then $N_f = 1$ and the mode for the frame at $\omega = \omega^*$ has neither $|\mathbf{K}(\omega)| = 0$ nor $\mathbf{D} = \mathbf{0}$. Note that cases C and D above and also the F–F bar case are all simple cases satisfying the rules given here.

To verify this conclusion numerically the rigidly jointed plane frame shown in Figure 6 was analyzed using a computer program [9] that uses the W–W algorithm. First, this program was modified to include an automated trial-and-error process to find a value of α for which the frame had a natural frequency ω^* at exactly the fundamental natural frequency of member 2–3 with C–C ends. This gave $\omega^* = 0{\cdot}1242961362$ rad/s and $\alpha = 1{\cdot}33402131574624$. This value of α was then altered by a succession of small amounts, to give $|\mathbf{K}(\omega)|$ versus ω plots very similar to Figure 5(b), but for which $|\mathbf{K}(\omega)| = -0{\cdot}53208955 \times 10^{23}$ at $\omega = \omega^*$.

6. CONCLUSIONS

It has been shown in the literature that for transcendental eigenvalue problems, the natural frequencies usually occur with $|\mathbf{K}(\omega)| = 0$ and otherwise can occur for $\mathbf{D} = \mathbf{0}$ and

$|\mathbf{K}(\omega)| \to \infty$. One situation in which the latter case was shown to occur is for structures which have a number, N_1, of identical members and which also have N_2 ($\geqslant 1$) natural frequencies that coincide with a C–C natural frequency of such members. The literature [2, 4, 5] covers the case $N_2 < N_1$ for plane frames and it is shown that the W–W algorithm correctly predicts the presence of the N_2 natural frequencies of the structure. It is also shown that this is the limiting case of N_2 very close natural frequencies at which $|\mathbf{K}(\omega)| = 0$ occurring when the N_1 members are very slightly different from one another, because then the $|\mathbf{K}(\omega)|$ versus ω curve has N_1 very close poles (i.e., vertical asymptotes) between which the N_2 zeros of the natural frequencies are sandwiched. Finally, it was noted from the computed results in the literature that, as the poles and zeros coalesced due to the N_1 members becoming identical, the end result was that the curve had a pole at the natural frequency. Hence the conclusion was drawn that $\mathbf{D} = \mathbf{0}$ modes corresponded to $|\mathbf{K}(\omega)| \to \infty$.

In the terms of the present paper, this situation can be stated as 'there is a pole of multiplicity $N_1 - N_2$ due to N_2 of the poles having been cancelled by the N_2 zeros'. Hence the previously neglected situation explored in the present paper, namely natural frequencies occurring for which $|\mathbf{K}(\omega)| \neq 0$, $\mathbf{D} \neq \mathbf{0}$ and $|\mathbf{K}(\omega)| \not\to \infty$, can be regarded as the limiting case in which $N_1 = N_2 = N$ and hence the poles and roots exactly cancel each other out. The analytical and numerical studies of the present paper have shown that $|\mathbf{K}(\omega)|$ has neither a zero nor a pole at such natural frequencies, so that it is not possible to locate them by following a plot of $|\mathbf{K}(\omega)|$. However, it is well known that the W–W algorithm enables computer programs to find these and all other natural frequencies with certainty even in the most adverse circumstances.

This paper has illustrated that the algorithm is also very effective for explaining unusual or unexpected analytical results, for example those for the simple bar examples presented, and can also be used to predict such special cases and the circumstances under which they will occur. In particular, it has been predicted that if any structure has N_f($\geqslant 1$) natural frequencies which coincide with each other and with N_f C–C natural frequencies of component members of the structure, then these natural frequencies will not exhibit any of $|\mathbf{K}(\omega)| = 0$, $\mathbf{D} = \mathbf{0}$ or $|\mathbf{K}(\omega)| \to \infty$. A numerical example involving a rigidly jointed plane frame with eight members, as well as the bar examples, confirmed this prediction for $N_f = 1$.

A numerical method for finding the modes corresponding to the natural frequencies of structures has been applied analytically to the simple bar examples presented. Hence it has been demonstrated that this method, which uses a fictitious random force vector, is very effective for obtaining modes to engineering accuracy and better even for the situation in which $|\mathbf{K}(\omega)| \neq 0$, $\mathbf{D} \neq \mathbf{0}$ and $|\mathbf{K}(\omega)| \not\to \infty$ at the natural frequency.

ACKNOWLEDGMENTS

The authors are grateful to the U.K. Engineering and Physical Sciences Research Council for support under grant number GR/R05406/01, to the National Natural Science Foundation of China and to the Royal Academy of Engineering for support during the first author's three-month stay at Tsinghua University and Dalian University of Technology in China, during which time this paper was written. The first author holds a chair at Cardiff University to which he will return upon completion of his appointment at City University of Hong Kong.

REFERENCES

1. F. W. WILLIAMS and W. H. WITTRICK 1970 *International Journal of Mechanical Sciences* **12**, 781–791. An automatic computational procedure for calculating natural frequencies of skeletal structures.

2. W. H. WITTRICK and F. W. WILLIAMS 1971 *Quarterly Journal of Mechanics and Applied Mathematics* **24**, 263–284. A general algorithm for computing natural frequencies of elastic structures.
3. W. H. WITTRICK and F. W. WILLIAMS 1973 *Journal of Structural Mechanics* **1**, 497–518. An algorithm for computing critical buckling loads of elastic structures.
4. H. R. RONAGH, R. LAWTHER and F. W. WILLIAMS 1995 *Journal of Engineering Mechanics, American Society of Civil Engineers* **121**, 948–955. Calculation of eigenvectors with uniform accuracy.
5. K. L. CHAN and F. W. WILLIAMS 2000 *Shock and Vibration* **7**, 23–28. Orthogonality of modes of structures when using the exact transcendental stiffness matrix method.
6. F. W. WILLIAMS 1978 *Computers and Structures* **9**, 427–429. A pocket calculator program for some simple vibration problems.
7. C. T. HOPPER and F. W. WILLIAMS 1977 *Journal of Structural Mechanics* **5**, 255–278. Mode finding in non-linear structural eigenvalue calculations.
8. F. W. WILLIAMS 1993 *Computers and Structures* **48**, 547–552. Review of exact buckling and frequency calculations with optional multi-level substructuring.
9. W. P. HOWSON 1979 *Advances in Engineering Software* **1**, 181–190. A compact method for computing the eigenvalues and eigenvectors of plane frames.